PD-0529: CT image features associated with patient-rated xerostomia after radiotherapy for head and neck cancer

Wagenaar, D.; Schaaf, A. Van der; Sijtsema, N.M.; Dijk, L.V. Van; Langendijk, J.A.; Steenbakkers, R.J.H.M.; Brouwer, C.L.

DOI:
10.1016/S0167-8140(15)40524-9

planning objectives, drawn from a Gaussian distribution with the base plan objective as mean and a pre-defined standard deviation, were automatically generated using worst-case scenario optimisation. Plans were evaluated on robustness by selecting the single-worst of 12 simulated perturbation scenarios based on density (3%) and position (8 mm in all directions) errors. For the plans fulfilling all minimal requirements after robustness evaluation, the PF was estimated based on the dominating plans for which one objective of interest cannot be improved without deteriorating other evaluation objectives of interest. To iteratively improve the PF estimate, a new base plan was automatically created using average planning objectives of dominating plans for a next iteration. After 5 iterations with 20 plans each, dominating plans were determined to form the 2D PF. Per patient, PFs based on different beam set-ups were compared by investigating trade-off differences between objectives of interest.

Table: Beam set-ups, planning objectives and evaluation objectives used. Asterisks indicate evaluation objectives of interest.

Beam set-up	*Gantry angles (°)*
2 beams	90, 270
3 beams	0, 90, 270
4 beams	30, 90, 270, 330
Planning objectives	
CTV	Minimal dose 46 Gy (w=120)
	Maximal dose 46.8 Gy (w=80; σ=50)
Body	Dose fall-off: 46–31 Gy over 1.0 cm (σ=0.6 cm) (w=100; σ=60)
Rectum	Maximal 30 Gy to 50% (σ=10%) of the volume (w=30; σ=10)
Minimal evaluation requirements	
CTV	At least 40 Gy received by 99% of the volume *
	At most 50.4 Gy received by 2% of the volume
Body	At most 1800 cm^3 receiving 43.7 Gy
Rectum	At most 90% of the volume receiving 30 Gy *
Bowel	At most 600 cm^3 receiving 45 Gy
Bladder	At most 75% of the volume receiving 45 Gy

Abbreviations: CTV=clinical target volume, Gy=Gray, w=weight, σ=standard deviation, cm=centimetre, cm^3=cubic centimetre.

Results: In total, 825 robustly optimised IMPT plans were automatically created and evaluated within 550 hours. Per derived PF, on average 25 plans (range, 11–45) did not fulfil all requirements and 15 dominating plans (range, 13–18) were found. The figure shows an example of dominating plans that form the PF (A) and PFs based on different beam set-ups used for comparison (B). For 2 out of 3 patients, PF comparison indicated a better trade-off between CTV D99% and rectum V30Gy for robust IMPT plans using 4 beams.

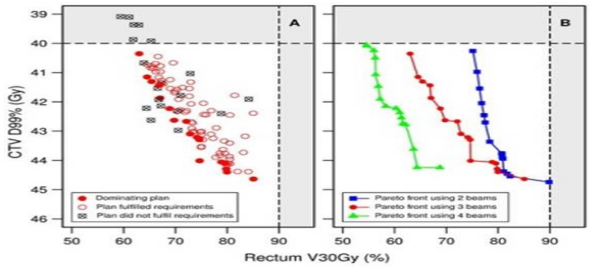

Figure: Single-worst perturbed scenarios of robustly optimised IMPT plans based on the 3-beam set-up of one patient (A), with plans that did not fulfil (black crossed dots) and plans that did fulfil (red dots) all requirements after robustness evaluation and dominating plans that form the Pareto front (filled red dots). Pareto fronts for robust IMPT plans based on a set-up using 2 beams (blue, squares), 3 beams (red, dots) and 4 beams (green, triangles) of one patient are shown (B).

Conclusions: A novel method to iteratively determine PFs based on robustly optimised IMPT plans including robustness evaluation was successfully scripted in RayStation. We demonstrated the feasibility of beam set-up comparison using PFs for proton therapy planning in cervical cancer.

PD-0529

CT image features associated with patient-rated xerostomia after radiotherapy for head and neck cancer

D. Wagenaar[1], A. Van der Schaaf[1], N.M. Sijtsema[1], L.V. Van Dijk[1], J.A. Langendijk[1], R.J.H.M. Steenbakkers[1], C.L. Brouwer[1]

[1]University Medical Center Groningen University of Groningen, Radiotherapy, Groningen, The Netherlands

Purpose/Objective: Xerostomia is the most frequently reported side effect of radiotherapy in head and neck cancer and has a major impact on quality of life. Current measurements of xerostomia are either subjective or unpleasant for the patient. We hypothesize that volume and density of the parotid and submandibular glands, which can be objectively determined from CT-scans, are related to their function and can therefore be used as image biomarkers for xerostomia. To test this hypothesis, we investigated the association of these image features with patient-rated xerostomia.

Materials and Methods: This prospective study included 110 patients with head and neck cancer who were treated with radiotherapy. Patient-rated xerostomia was scored on a 4-point Likert scale using the EORTC QLQ-H&N35 questionnaire 12 weeks after treatment start (Xer_{12wk}) and 6 months after treatment (Xer_{6m}). In addition, CT-scans were made at baseline and 12 weeks after treatment. The CT density (in HU), volume (in cm^3) and their change between both CT-scans were calculated for the parotid and submandibular glands. Associations with Xer_{12wk} and Xer_{6m} were calculated using univariable and multivariable linear regression and Pearson correlation (r).

Results: In the univariable analysis a statistically significant relation was found between Xer_{12wk} and change in volume of the parotid glands and change in density of the submandibular glands between the CT-scans at baseline and 12 weeks after treatment (Table 1). Furthermore, a statistically significant relation was found between Xer_{6m} and change in and density of the parotid glands and change in density of the submandibular glands.

Table 1: Univariable linear regression relating CT image feature changes to patient-rated xerostomia after 12 weeks and 6 months.

	Coefficient	p-value	Correlation coefficient
Associations with Xerostomia ,12 weeks after treatment start			
Parotid glands volume change (cm^3)	-0.039	<0.001	-0.367
Submandibular glands density change (HU)	-0.006	0.042	0.200
Associations with xerostomia 6 months after end of treatment			
Parotid glands volume change (cm^3)	-0.039	<0.001	-0.362
Parotid glands density change (HU)	-0.010	0.001	-0.309
Submandibular glands density change (HU)	-0.011	<0.001	-0.355

Figure 1: Boxplots for the volume and density change of the parotid glands and the density change of the submandibular glands after 12 weeks for patients with or without patient-rated xerostomia after 6 months.

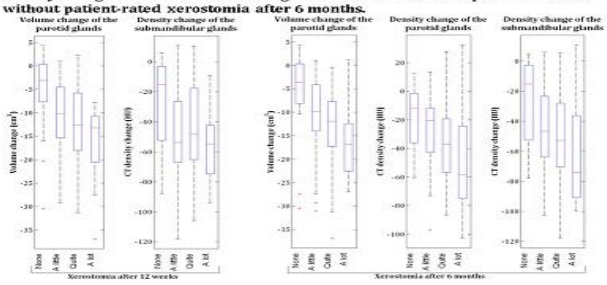

At baseline, a high density of the parotid (β = 0.004, p = 0.03, r = 0.22) and submandibular glands (β = 0.004, p = 0.05, r = 0.20) were predictive for Xer_{6m}. No baseline features were significantly associated with Xer_{12wk}.

In the multivariable model the change in volume of the parotid glands and change in density of the submandibular

glands were independently associated with Xer_{6m}, with a correlation coefficient of 0.454 between the model predictions and Xer_{6m}. No multivariable model with multiple significant independent predictors was found for Xer_{12wk}.
A significant correlation between Xer_{6m} and Xer_{12wk} was found with a correlation coefficient of 0.627
Conclusions: The volume and density of the parotid glands and the density of the submandibular glands are associated with xerostomia after radiotherapy. The changes of these CT image features over the course of treatment are more strongly related to xerostomia than the instantaneous feature values at baseline. Moreover, the feature changes in the first 12 weeks after start of treatment are equally or even more strongly related to xerostomia at 6 month than at 12 weeks. These associations suggest that, even early after treatment, the CT image feature changes may be used as objective biomarkers of the development of xerostomia.

PD-0530

Predictors of hematological toxicity after whole-pelvis intensity-modulated post-prostatectomy radiotherapy

C. Sini[1], C. Fiorino[1], B. Noris Chiorda[2], A. Chiara[2], C. Deantoni[2], C. Gumina[2], L. Perna[1], A. Sbalchiero[2], R. Calandrino[1], N. Di Muzio[2], C. Cozzarini[2]
[1]San Raffaele Scientific Institute, Medical Physics Department, Milan, Italy
[2]San Raffaele Scientific Institute, Radiotherapy Department, Milan, Italy

Purpose/Objective: Hematologic toxicity (HT) is an important side-effect of whole pelvis intensity-modulated radiotherapy (WP-IMRT), but association between radiation dose and HT remains unclear when concurrent chemotherapy is not prescribed. The aim of this study was to identify clinical and dosimetric predictors of HT in a cohort of chemo-naÏf patients treated with WPRT.
Materials and Methods: The first 121 patients enrolled in a prospective observational study, treated with adjuvant (n=72) or salvage (n=49) WP-IMRT in a single Institute were available (static field IMRT: 19; VMAT/Rapidarc:57; Helical Tomotherapy:45). Pelvic bones, used as a surrogate for pelvic bone marrow (BM), were contoured according to Mell et al [IJROBP 2006] and divided in four subvolumes: ilium (IL), lumbosacral spine (LS), lower pelvis (LP) and whole pelvis (WP). The volume of each BM region receiving 3, 5, 10, 20, 30, 40 and 50 Gy (V3-50) was recovered. Absolute values of lymphocytes (ALC), white blood cell (WBC) and neutrophils (N) were prospectively collected before WPRT, at half WPRT, at end WPRT, at 3m and at 12 months after WPRT. HT was graded according to CTCAE v. 3.0: Grade 3 (G3) and Grade 1 (G1) events were considered as end-points for acute (nadir value) and late HT respectively. Uni- and backward multi-variable logistic regression was performed to assess correlation between clinical/DVH parameters and HT. A previously introduced method based on DVH differences between patients with/without HT was used to select the most discriminative DVH parameters.
Results: The nadir of WBC and N (median values= 65% and 74% of baseline respectively) was found at half-therapy while it was at the end of RT for ALC (median= 30% of baseline). No patients showed acute G3 neither late G1 WBC and N toxicities. Interestingly, the mean value of ALC at 1 year was 54% of baseline: 28 acute G3 and 14 late G1 lymphopenias were found. Then, the analysis was restricted to ALC at the end of therapy (ALCend) and at 12 months (ALC12m). At univariate analysis, a lower baseline ALC (ALCbase) was correlated with G3 ALCend and G1 ALC12m (p=0.003 and p<0.001, respectively). Concerning dosimetric parameters, IL-V30/IL-V40 and WP-V40 were correlated with acute G3 ALCend and late G1 ALC12m (p=0.003). The resulting model for ALCend included ALCbase and WP-V40 (AUC =0.73); the model for ALC12m included ALCbase and IL-V40 (AUC= 0.82). Best cut-off values (assessed by ROC) discriminating patients with/without lymphopenia were: ALCbase ≤1830 x 10(9)/L and WP-V40 >599.4 cc (G3 ALCend); ALCbase ≤1780 x 10(9)/L and IL-V40>94.6 cc (G1 ALC12m) (Fig-1).

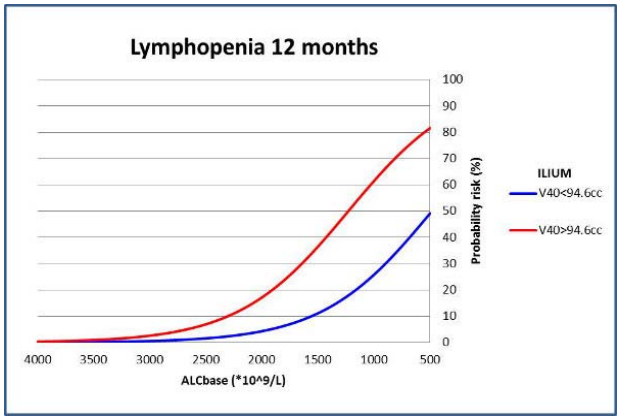

Conclusions: Two-variable models including ALCbase and DVH parameters of pelvic BM may predict acute G3 and late G1 lymphopenia after WP-IMRT in post-prostatectomy RT. The model could be used to reduce HT by constraining BM. Further validation on a larger population is ongoing.

PD-0531

Dosimetric investigation of rotational setup errors for spine stereotactic radiosurgery: a phantom study

M. Sasaki[1], M. Nakamura[2], N. Mukumoto[2], M. Nakata[1], K. Higashimura[1], M. Hiraoka[2]
[1]Kyoto University Hospital, Clinical Radiology Service, Kyoto, Japan
[2]Kyoto University Graduate School of Medicine, Radiation Oncology and Image-applied Therapy, Kyoto, Japan

Purpose/Objective: A final accuracy of positioning < 2 mm is the recommended tolerance level for image-guided radiotherapy (IGRT) for spine stereotactic radiosurgery (SRS) in RTOG 0631. However, the tolerance level for rotation is not specified. This study investigated experimentally the effect of rotational setup errors on dose distribution for spine SRS.
Materials and Methods: The contour definitions and treatment planning were as per RTOG 0631. A 16-Gy dose was prescribed in a single fraction by step-and-shoot intensity-modulated radiation therapy (IMRT) using seven coplanar beams with the Vero4DRT (Mitsubishi Heavy Industries, Ltd., Hiroshima, Japan, and Brainlab AG, Feldkirchen, Germany). An isocenter was placed inside the vertebral body. Setup error patterns were categorized into three groups. Only translational errors were generated for Group A, with the translational errors measuring +1, +2, +3, and +5 mm in the lateral (LAT), longitudinal (LNG), and vertical (VRT) directions, respectively. Only rotational errors were generated for Group B, and measured +1°, +2°, +3°, and +5° in terms of the tilt or roll angle. Combinations of translational and rotational errors occurred in Group C. Translational errors of 0 to 2 mm were generated in each direction and rotational errors of ±1° or ±2° in each direction. Data were acquired with a Delta4 phantom (ScandiDos, Uppsala, Sweden) and setup errors were generated with HexaMotion (ScandiDos, Uppsala, Sweden).